

Rhodium Acetylacetonate and Iron Tricarbonyl Complexes of Tetracyclone and 3-Ferrocenyl-2,4,5-triphenylcyclopentadienone: An X-ray Crystallographic and NMR Study

Hari K. Gupta, Nicole Rampersad, Mark Stradiotto, and Michael J. McGlinchey*

Department of Chemistry, McMaster University, Hamilton, Ontario L8S 4M1, Canada

Received July 19, 1999

Tetracyclone reacts with $\text{Fe}_2(\text{CO})_9$ and with $(\text{acac})\text{Rh}(\text{C}_2\text{H}_4)_2$ to give $(\text{C}_4\text{Ph}_4\text{C}=\text{O})\text{Fe}(\text{CO})_3$ (**3**) and $(\text{C}_4\text{Ph}_4\text{C}=\text{O})\text{Rh}(\text{acac})$ (**11**), respectively. Likewise, 3-ferrocenyl-2,4,5-triphenylcyclopentadienone (**2**) yields $(\text{C}_4\text{Ph}_3\text{FcC}=\text{O})\text{Fe}(\text{CO})_3$ (**7**) and $(\text{C}_4\text{Ph}_3\text{FcC}=\text{O})\text{Rh}(\text{acac})$ (**14**). In **3**, the peripheral phenyl substituents adopt a propeller conformation in the solid state, and the barrier to fluxionality of the $\text{Fe}(\text{CO})_3$ fragment is so low as to preclude the observation of slowed tripodal rotation at low temperature. In contrast, the ferrocenyl analogue **7** shows restricted tripodal rotation, but this may be the result of steric interference by the bulky ferrocenyl substituent. In the crystal, (tetracyclone) $\text{Rh}(\text{acac})$ (**11**) exists as a head-to-tail dimer in which the rhodium center is bonded to the γ -carbon of the acetylacetonate ligand in the other half of the molecule. The ferrocenyl analogue **14** is monomeric both in the solid state and in solution, and the rotation barrier of the $\text{Rh}(\text{acac})$ fragment has been evaluated as 12 kcal mol⁻¹. The mass spectra of the rhodium complexes are discussed in terms of doubly charged ions containing $\text{Rh}(\text{III})$. The potential use of these metal-complexed cyclopentadienones as precursors to pentaaryl cyclopentadienyl systems is discussed.

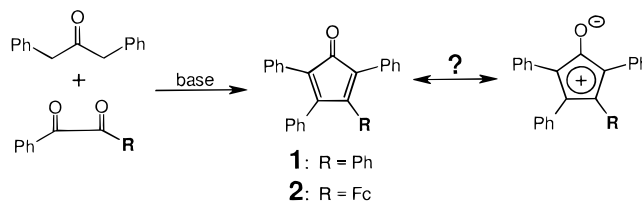
Introduction

While metal complexes of cyclopentadienones are very numerous, the majority of these species arose as minor products from the reactions of alkynes with metal carbonyls.¹ However, cyclopentadienones are also available by direct synthesis from appropriately designed benzils and 1,3-disubstituted propanones,² as shown in Scheme 1.

A crucial factor controlling the chemistry of cyclopentadienones is the relatively small HOMO–LUMO gap,³ as evidenced by their intense visible absorption and strong tendency to undergo Diels–Alder dimerization unless hindered by the presence of bulky substituents.² In these systems, the carbonyl group is considered to be relatively nonpolarized, since the zwitterionic resonance structure depicted in Scheme 1 would invoke a four- π -electron manifold with antiaromatic character.⁴

The ready availability of monomeric tetracyclone (2,3,4,5-tetraphenylcyclopentadienone, **1**) has prompted the preparation of a number of organometallic derivatives,^{5–12} as exemplified in Scheme 2, which also shows some complexes derived from diphenylacetylene.

Scheme 1. Synthetic Route to Cyclopentadienones



Our current focus on metal complexes of cyclopentadienones bearing bulky substituents derives from our long-standing interest in $(\text{C}_x\text{Ar}_x)\text{ML}_n$ systems, where $x = 5,^{13} 6,^{14}$ or $7,^{15}$ and their relevance to correlated rotations.¹⁶ We here describe the syntheses, structures,

* To whom correspondence should be addressed. Phone: (905) 525-9140 ext. 24504. Fax: (905) 522-2509. E-mail: mcglinch@mcmaster.ca.

(1) Adams, H.; Bailey, N. A.; Hempstead, P. D.; Morris, M. J.; Riley, S.; Beddoes, R. L.; Cook, E. S. *J. Chem. Soc., Dalton Trans.* **1993**, 91.

(2) (a) Allen, C. F. H. *Chem. Rev.* **1962**, 62, 653. (b) Ogliaruso, M. A.; Romanelli, M. G.; Becker, E. I. *Chem. Rev.* **1965**, 65, 261.

(3) Garbisch, E. W., Jr.; Sprecher, R. F. *J. Am. Chem. Soc.* **1969**, 91, 6785 and references therein.

(4) Bergmann, E. D.; Berthier, G.; Ginsburg, D.; Hirschberg, Y.; Lavie, D.; Pinchas, S.; Pullman, B.; Pullmann, A. *Bull. Soc. Chim. Fr.* **1951**, 18, 661.

(5) (a) Schrauzer, G. N. *J. Am. Chem. Soc.* **1959**, 81, 5307. (b) Weiss, E.; Hübel, W. *J. Inorg. Nucl. Chem.* **1959**, 11, 42.

(6) (a) Bruce, M. I.; Knight, J. R. *J. Organomet. Chem.* **1968**, 12, 411. (b) Blum, Y.; Shvo, Y.; Chodosh, D. F. *Inorg. Chim. Acta* **1985**, 97, L25. (c) Bailey, N. A.; Jassal, V. S.; Vefghi, R.; White, C. *J. Chem. Soc., Dalton Trans.* **1987**, 2815.

(7) Baker, P. K.; Broadley, K.; Connelly, N. G.; Kelly, B. A.; Kitchen, M. D.; Woodward, P. *J. Chem. Soc., Dalton Trans.* **1980**, 1710.

(8) (a) Markby, R.; Sternberg, H. W.; Wender, I. *Chem. Ind.* **1959**, 1387. (b) Sheats, J. E.; Rausch, M. D. *J. Org. Chem.* **1970**, 35, 3245.

(9) McVey, S. P.; Maitlis, P. M. *Can. J. Chem.* **1966**, 44, 2429.

(10) Dickson, R. S.; Tailby, G. R. *Aust. J. Chem.* **1970**, 23, 1531.

(11) Pasynskii, A. A.; Anisimov, K. N.; Kolobova, N. E.; Nesmeyanov, A. N. *Dokl. Akad. Nauk SSSR* **1969**, 185, 610.

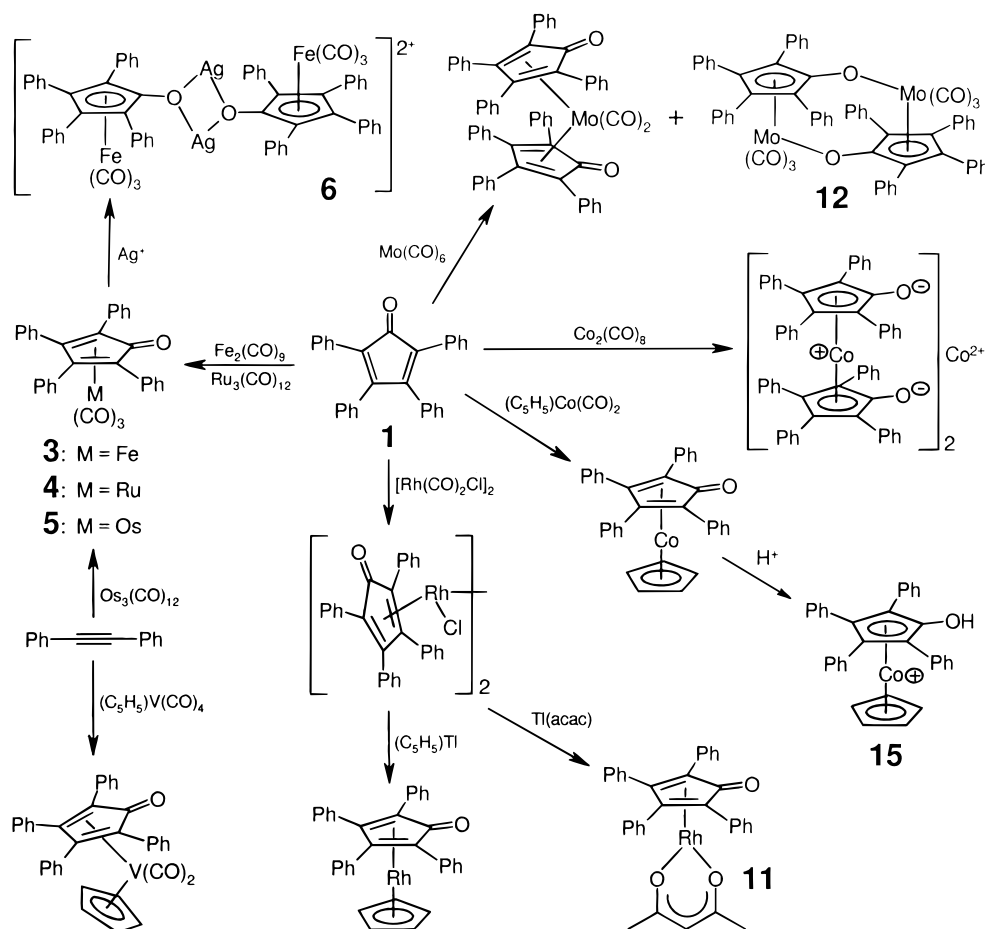
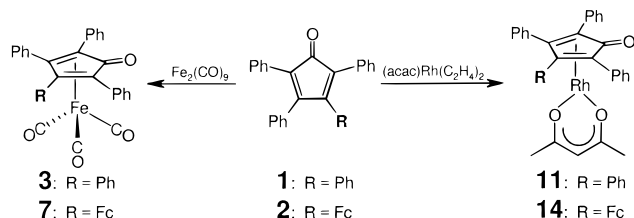
(12) Burke, M. R.; Funk, T.; Takats, J. *Organometallics* **1994**, 13, 2109.

(13) Li, L.; Decken, A.; Sayer, B. G.; McGlinchey, M. J.; Brégaire, P.; Thépot, J.-Y.; Toupet, L.; Hamon, J.-R.; Lapinte, C. *Organometallics* **1994**, 13, 682.

(14) Mailvaganam, B.; Sayer, B. G.; McGlinchey, M. J. *J. Organomet. Chem.* **1990**, 395, 177.

(15) (a) Chao, L. C. F.; Gupta, H. K.; Hughes, D. W.; Britten, J. F.; Rigby, S. S.; Bain, A. D.; McGlinchey, M. J. *Organometallics* **1995**, 14, 1139. (b) Brydges, S.; Gupta, H. K.; Chao, L. C. F.; Pole, D. L.; Britten, J. F.; McGlinchey, M. J. *Chem. Eur. J.* **1998**, 4, 1201.

Scheme 2. Metal Complexes of Tetracyclone

Scheme 3. Reactions of 1 and 2 with $\text{Fe}_2(\text{CO})_9$ and $(\text{acac})\text{Rh}(\text{C}_2\text{H}_4)_2$ 

and molecular dynamics of $\text{Fe}(\text{CO})_3$ and $\text{Rh}(\text{acac})$ derivatives of tetracyclone (**1**) and of 3-ferrocenyl-2,4,5-triphenylcyclopentadienone (**2**).

Results and Discussion

$\text{Fe}(\text{CO})_3$ Complexes. As previously described,⁵ tetracyclone and $\text{Fe}_2(\text{CO})_9$ yield the complex $(\text{C}_4\text{Ph}_4\text{C}=\text{O})\text{Fe}(\text{CO})_3$ (**3**; Scheme 3), whose infrared and ^{13}C NMR spectra have already been reported.¹² The X-ray crystal structure of **3** is shown as Figure 1 and clearly illustrates the η^4 character of the bonding of the tripodal group to the cyclic ligand; crystallographic refinement parameters and selected metrical data are collected in Tables 1 and 2, respectively. The average bonding distance from the iron to the tetracyclone ring carbons C(2)–C(5) is 2.14 Å and is markedly shorter than the distance to the ketonic carbon ($\text{Fe}–\text{C}(1) = 2.40(1)$ Å). There is no evidence of carbon–carbon bond alternation

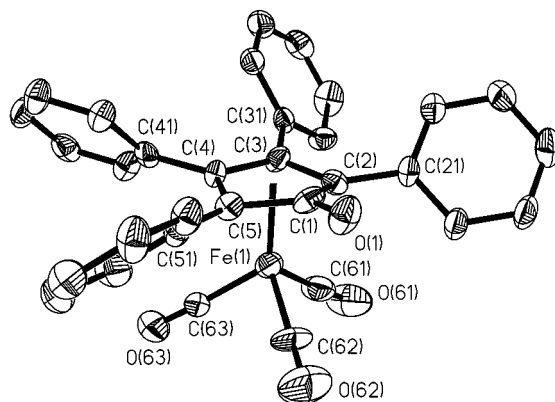


Figure 1. Molecular structure of $(\text{C}_4\text{Ph}_4\text{C}=\text{O})\text{Fe}(\text{CO})_3$ (**3**; 25% thermal ellipsoids), with hydrogen atoms omitted for clarity.

within the diene system, and overall the pattern is typical of those reported for a variety of $(\eta^4\text{-diene})\text{Fe}(\text{CO})_3$ structures.¹⁷ Moreover, the carbonyl moiety within the five-membered ring does not lie in the plane defined by C(2), C(3), C(4), and C(5), but, rather, is displaced through 16° away from the metal. As in other sterically crowded systems,¹⁸ the peripheral aryl rings in **3** adopt

(17) Deeming, A. J. In *Comprehensive Organometallic Chemistry*; Wilkinson, G., Stone, F. G. A., Abel, E. W., Eds.; Pergamon: Oxford, U.K., 1982; Vol. 4, Chapter 31.3, pp 449–450.

(18) (a) Adams, H.; Bailey, N. A.; Browning, A. F.; Ramsden, J. A.; White, C. J. *Organomet. Chem.* **1990**, *387*, 305. (b) Harrison, W. M.; Saadeh, C.; Colbran, S. B.; Craig, D. C. *J. Chem. Soc., Dalton Trans.* **1997**, 3785 and references therein.

(16) Iwamura, H.; Mislow, K. *Acc. Chem. Res.* **1988**, *21*, 175.

Table 1. Crystallographic Collection and Refinement Parameters for 3·THF, 7, 11·H₂O and 14

	3·THF	7	11·H ₂ O	14
empirical formula	C ₃₆ H ₂₈ O ₅ Fe	C ₃₆ H ₂₄ O ₄ Fe ₂	C ₃₄ H ₂₉ O ₄ Rh	C ₃₈ H ₃₁ O ₃ FeRh
mol wt	596.43	632.25	604.48	694.39
descripn	red prism	dark red prism	red prism	red prism
size, mm ³	0.30 × 0.21 × 0.13	0.38 × 0.34 × 0.25	0.12 × 0.09 × 0.06	0.24 × 0.20 × 0.17
temp, K	299(2)	299(2)	299(2)	299(2)
cryst syst	monoclinic	monoclinic	triclinic	monoclinic
space group	<i>P</i> 2 ₁ / <i>c</i>	<i>P</i> 2 ₁ / <i>n</i>	<i>P</i> 1	<i>P</i> 2 ₁ / <i>a</i>
<i>a</i> , Å	10.623(9)	10.618(3)	8.823(9)	20.834(9)
<i>b</i> , Å	11.739(9)	21.506(6)	12.404(4)	12.455(7)
<i>c</i> , Å	24.89(2)	12.990(3)	15.694(5)	25.75(2)
α, deg	90	90	66.929(7)	90
β, deg	102.28(1)	102.33(1)	81.291(8)	97.09(2)
γ, deg	90	90	73.873(6)	90
<i>V</i> , Å ³	3032(4)	2898(1)	1516.2(8)	6631(7)
<i>Z</i>	4	4	2	8
calcd density, g/cm ³	1.306	1.449	1.324	1.391
scan mode	<i>ω</i> -scans	<i>ω</i> -scans	<i>ω</i> -scans	<i>ω</i> -scans
<i>F</i> (000)	1240	1296	620	2832
abs coeff, mm ⁻¹	0.539	1.041	0.597	0.969
θ range, deg	1.67–22.50	1.86–23.50	1.41–23.50	1.59–23.50
index ranges	–12 ≤ <i>h</i> ≤ 13 –14 ≤ <i>k</i> ≤ 14 –29 ≤ <i>l</i> ≤ 30	–12 ≤ <i>h</i> ≤ 13 –27 ≤ <i>k</i> ≤ 25 –16 ≤ <i>l</i> ≤ 16	–11 ≤ <i>h</i> ≤ 6 –14 ≤ <i>k</i> ≤ 16 –19 ≤ <i>l</i> ≤ 20	–26 ≤ <i>h</i> ≤ 24 –16 ≤ <i>k</i> ≤ 14 –33 ≤ <i>l</i> ≤ 33
no. of rflns collected	18 186	19 222	6445	19 560
no. of indep rflns	3972	4282	4396	4897
no. of data/restraints/params	3955/3/356	4280/0/380	4391/0/361	4889/0/388
GOF on <i>F</i> ² (all)	0.909	0.909	1.520	0.913
final <i>R</i> (<i>I</i> > 2σ(<i>I</i>))	<i>R</i> 1 = 0.0944; w <i>R</i> 2 = 0.2008	<i>R</i> 1 = 0.0283; w <i>R</i> 2 = 0.0663	<i>R</i> 1 = 0.1161; w <i>R</i> 2 = 0.3339	<i>R</i> 1 = 0.0478; w <i>R</i> 2 = 0.0997
<i>R</i> indices (all data)	<i>R</i> 1 = 0.2075; w <i>R</i> 2 = 0.2594	<i>R</i> 1 = 0.0506; w <i>R</i> 2 = 0.0721	<i>R</i> 1 = 0.1330; w <i>R</i> 2 = 0.3462	<i>R</i> 1 = 0.0940; w <i>R</i> 2 = 0.1123
transmissn, (max, min)	0.9630, 0.5106	0.7340, 0.6331	0.9821, 0.6422	0.9131, 0.5904
largest diff peak, e/Å ³	0.565	0.188	2.842	0.500
largest diff hole, e/Å ³	–0.602	–0.204	–0.733	–0.414

Table 2. Selected Bond Lengths (Å) and Angles (deg) for 3·THF, 7, 11·H₂O, 14, and Related Structures

	3	4 ^b	5 ^c	7	11	14
M–C(5) ^a	2.167(9)	2.240(3)	2.230(11)	2.136(3)	2.165(12)	2.165(6)
M–C(4)	2.126(8)	2.209(3)	2.231(12)	2.061(2)	2.123(11)	2.098(5)
M–C(3)	2.117(9)	2.216(3)	2.199(12)	2.112(2)	2.135(12)	2.139(5)
M–C(2)	2.147(9)	2.216(3)	2.265(11)	2.108(2)	2.166(12)	2.149(5)
M–C(1)	2.402(13)	2.530(3)	2.563(10)	2.422(3)	2.420(13)	2.380(6)
C(1)–O(1)	1.216(11)	1.224(4)	1.207(15)	1.226(3)	1.21(2)	1.227(7)
C(5)–C(4)	1.42(1)	1.438(4)	1.480(18)	1.449(3)	1.46(2)	1.423(7)
C(1)–C(5)	1.52(1)	1.491(4)	1.509(16)	1.479(3)	1.46(2)	1.495(8)
C(3)–C(4)	1.46(1)	1.437(4)	1.428(15)	1.444(3)	1.44(2)	1.468(7)
C(2)–C(3)	1.47(1)	1.455(4)	1.456(17)	1.435(3)	1.45(2)	1.425(7)
C(1)–C(2)	1.47(1)	1.485(4)	1.546(15)	1.478(3)	1.51(2)	1.482(8)
C(5)–C(4)–C(3)	110.2(7)	108.9	107.1(10)	108.2(2)	107.3(11)	109.3(5)
C(4)–C(3)–C(2)	105.9(7)	107.2	111.6(10)	107.3(2)	108.7(11)	106.5(5)
C(3)–C(2)–C(1)	109.2(7)	108.0	105.1(9)	108.1(2)	107.4(10)	109.9(5)
C(2)–C(1)–C(5)	104.2(9)	103.2	103.5(9)	103.8(2)	104.2(10)	103.9(5)
C(5)–C(1)–O(1)	127.4(8)	129.6	127.8(10)	129.5(2)	128.7(13)	128.1(6)
C(2)–C(1)–O(1)	128.0(9)	126.9	128.5(10)	126.5(2)	126.4(13)	127.3(5)
fold angle ^d	16	19	20	21	17	13

^a M = Fe (**3**), Ru (**4**), Os (**5**), Fe (**7**), Rh (**11**), and Rh (**14**). ^b Reference 6b. ^c Reference 12. ^d The angle subtended by the planes defined by C(2)–C(3)–C(4)–C(5) and C(2)–C(1)–C(5).

a propeller conformation such that the average dihedral angle made by these phenyls and the central ring is ~49°.

These structural data should be compared to those of the analogous ruthenium^{6b} and osmium¹² complexes **4** and **5**, as listed in Table 2, which illustrate the close similarity in their propeller conformations; the *exo* fold angle of the ketonic unit ranges from 16° in the Fe system to ~20° in the Ru and Os complexes. Moreover, in the latter two systems, the alignment of the ring carbonyl with one of the M–CO linkages is almost perfect (dihedral angle ~8°); in contrast, the Fe(CO)₃

tripod in **3** is rotated by 28° away from the completely eclipsed position, probably for steric reasons.

The closest analogue of **3** to have been structurally characterized is the oxygen-bridged dication {[Fe(CO)₃-(*η*⁵-C₅Ph₄C–O–Ag)]₂}²⁺ (**6**), obtained by silver hexafluorophosphate oxidation of **3** and shown in Scheme 2.⁷ In the silver complex, the propeller-like orientation of the peripheral phenyls is maintained and the tripodal Fe(CO)₃ unit is rotated by 18° away from the eclipsed position, somewhat less than is found in **3**. However, the dimerization is not mediated simply via bridging of the ketonic oxygens to both silver atoms. While the

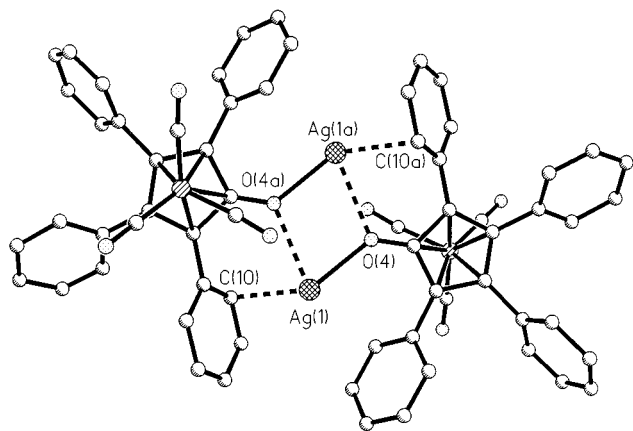


Figure 2. Structure of $\{[\text{Fe}(\text{CO})_3(\eta^5\text{-C}_5\text{Ph}_4\text{C=O-Ag})]_2\}^{2+}$ (**6**). Data were taken from ref 7.

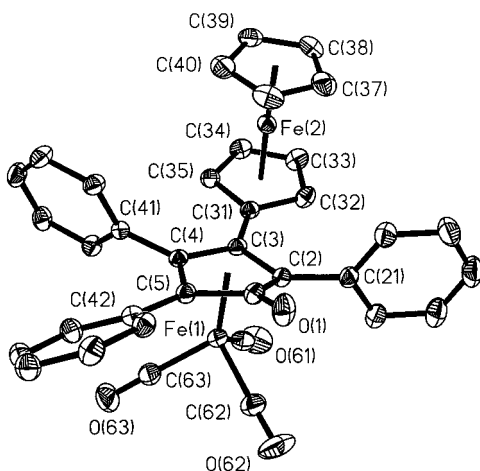


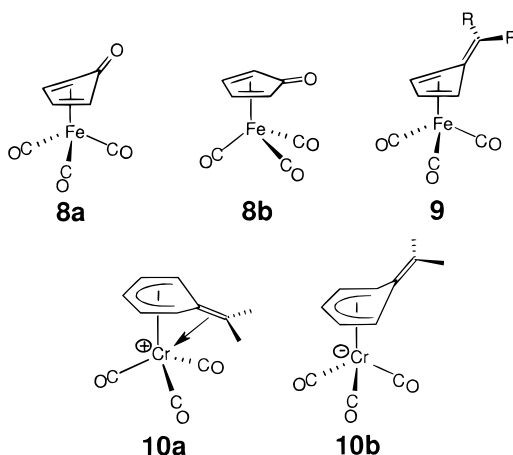
Figure 3. Molecular structure of $(\text{C}_4\text{Ph}_3\text{FcC=O})\text{Fe}(\text{CO})_3$ (**7**; 25% thermal ellipsoids), with hydrogen atoms omitted for clarity.

Ag(1)–O(4) and Ag(1)–O(4A) distances are 2.27(2) and 2.65(8) Å, respectively, each silver is also only 2.46(5) Å from a phenyl carbon, as depicted in Figure 2.

Treatment of a THF solution of 3-ferrocenyl-2,4,5-triphenylcyclopentadienone (**2**) with $\text{Fe}_2(\text{CO})_9$ yields **7**, the complex analogous to **3** whereby a peripheral phenyl substituent has been replaced by a ferrocenyl unit. While the major structural features of **7** (see Figure 3) resemble those of the $(\text{C}_4\text{Ph}_4\text{C=O})\text{M}(\text{CO})_3$ systems discussed above, the orientations of the peripheral phenyls are markedly different. The C_5H_4 ring of the ferrocenyl substituent is almost coplanar (dihedral angle $\sim 9.8^\circ$) with the central ring, thus causing considerable twisting of its phenyl neighbors away from the conventional propeller arrangement; we have previously noted a similar effect in ferrocenyl-pentaphenylbenzene, in which the peripheral phenyls adopt sequentially greater dihedral angles,¹⁹ perhaps implying some degree of correlated rotation. However, in the absence of extensive labeling experiments, such an assertion must remain speculative.

The observed orientation of the $\text{M}(\text{CO})_3$ tripod in these complexes can be rationalized by means of molecular orbital calculations²⁰ at the extended Hückel level which show not only that the eclipsed rotamer **8a** is favored

Chart 1



over the staggered isomer **8b** (Chart 1) by 5.7 kcal mol^{−1} but also that the ring ketonic unit should fold away from the metal through $\sim 10^\circ$. This latter phenomenon was briefly discussed by Hoffmann some years ago.²¹

Likewise, the calculational²² and X-ray crystallographic²³ evidence on the closely analogous (fulvene)- $\text{Fe}(\text{CO})_3$ system **9** reveals that the exocyclic C=CR_2 group eclipses a carbonyl ligand and is folded in a distal fashion relative to the metal.

It is interesting to compare these data with a very recent report describing high-level calculations on tri-carbonylchromium complexes of benzyl cations, anions, and radicals.²⁴ In that study it was concluded that the favored structure for the cation places the tripod in the staggered orientation **10a**, with the exocyclic $-\text{CH}_2^+$ substituent folded 37° toward the chromium atom. In contrast, the benzyl anion complex is predicted to adopt the eclipsed conformation **10b**, with the methylene substituent folded 18° away from the chromium atom, analogous to **8a**. Moreover, the barriers to tripodal rotation in the (benzyl) $\text{Cr}(\text{CO})_3$ cation and anion were calculated to be 11.2 and 5.9 kcal mol^{−1}, respectively. Gratifyingly, variable-temperature NMR measurements have yielded values of 11–12 kcal mol^{−1} for a series of $\text{Cr}(\text{CO})_3$ -complexed benzyl cations;²⁵ although the corresponding (benzyl) $\text{Cr}(\text{CO})_3$ anions have also been examined at low temperature,²⁶ the barriers are presumably so small as to prevent the observation of slowed tripodal rotation on the time scale of NMR line-shape measurements.

Previous attempts by Kruczynski and Takats to detect slowed tripodal rotation in $(\text{C}_4\text{Ph}_4\text{C=O})\text{M}(\text{CO})_3$, where $\text{M} = \text{Fe}$ (**3**), Ru (**4**), were unsuccessful;²⁷ in that study,

(20) High-level ab initio calculations have been carried out for $(\text{C}_4\text{H}_4\text{C=O})\text{Fe}(\text{CO})_3$ and for $(\text{C}_4\text{H}_4\text{C=O})\text{Co}(\text{C}_5\text{H}_5)$, but the main focus of the study was a comparison of the two isolobal ML_n fragments: Chinn, J. W., Jr.; Hall, M. B. *Organometallics* **1984**, *3*, 284.

(21) Hoffmann, R.; Hoffmann, P. *J. Am. Chem. Soc.* **1976**, *98*, 598.

(22) Albright, T. A.; Hoffmann, R.; Hoffmann, P. *Chem. Ber.* **1978**, *111*, 1591.

(23) In (6,6-diphenylfulvene) $\text{Fe}(\text{CO})_3$ the *exo* fold angle is 18.5° : Edelmann, F.; Lubke, B.; Behrens, U. *Chem. Ber.* **1982**, *115*, 1325.

(24) Pfletschinger, A.; Dargel, T. K.; Bats, J. W.; Schmalz, H.-G.; Koch, W. *Chem. Eur. J.* **1999**, *5*, 537.

(25) (a) Acampora, M.; Ceccon, A.; Dal Farra, M.; Giacometti, G.; Rigatti, G. *J. Chem. Soc., Perkin Trans. 2* **1977**, 483. (b) Downton, P. A.; Sayer, B. G.; McGlinchey, M. J. *Organometallics* **1992**, *11*, 3281.

(26) (a) Jaouen, G.; Top, S.; Sayer, B. G.; McGlinchey, M. J. *J. Am. Chem. Soc.* **1983**, *105*, 6426. (b) Ceccon, A.; Gambaro, A.; Venzo, A. *J. Organomet. Chem.* **1984**, *275*, 209.

(27) Kruczynski, L.; Takats, J. *Inorg. Chem.* **1976**, *15*, 3140.

(19) Gupta, H. K.; Brydges, S.; McGlinchey, M. J. *Organometallics* **1999**, *18*, 115.

^{13}C NMR spectra were obtained at 22.6 MHz on a 90 MHz instrument at 183 K. Moreover, these workers pointed out that the range of ^{13}CO chemical shifts in (cyclopentadienone) $\text{M}(\text{CO})_3$ systems is rather narrow;²⁷ nevertheless, we attempted to detect slowed rotation of the $\text{Fe}(\text{CO})_3$ moiety in **3**. However, even at 167 K on a 500 MHz instrument (^{13}C spectra acquired at 125 MHz) the $\text{Fe}(\text{CO})_3$ resonance in $(\text{C}_4\text{Ph}_4\text{C}=\text{O})\text{Fe}(\text{CO})_3$ remained as a sharp singlet. This observation suggests either that the barrier is rather low (as indicated by the EHMO calculations) or that the chemical shift difference between the carbonyl environments is very small. Solid-state ^{13}C NMR measurements on this and related systems will be described in a future report.

In contrast, when the ferrocenyl complex **7** was cooled to 177 K in CD_2Cl_2 , it gave rise to three equally intense resonances at 209.1, 207.2, and 207.0 ppm; the barrier was evaluated as $12.5 \pm 0.5 \text{ kcal mol}^{-1}$. Interestingly, over the temperature range 173–300 K, the ^1H and ^{13}C NMR spectra of **7** indicated the presence of two isomers in an approximate 80/20 ratio, as shown by the observation of two different ferrocenyl environments. Whether these represent two rotamers in which the ferrocenyl substituents occupy *exo* and *endo* positions remains an open question. The X-ray crystal structure clearly shows that, at least in the solid state, the *exo* rotamer is favored, but the situation in solution is less clear. It was not possible to detect the ^{13}CO resonances of the minor component.

Rh(acac) Complexes. In 1966, Maitlis described the synthesis of $(\text{C}_4\text{Ph}_4\text{C}=\text{O})\text{Rh}(\text{acac})$ **11**, which was obtained by treatment of the chlorine-bridged dimer $[(\text{C}_4\text{Ph}_4\text{C}=\text{O})\text{RhCl}]_2$ with thallium acetylacetonate.⁹ The current, more direct approach simply involved gentle reflux in THF of the appropriate ligand **1** or **2** with $(\text{acac})\text{Rh}(\text{C}_2\text{H}_4)_2$, in which the ethylene ligands are known to be readily replaceable.

Since the Rh–acetylacetonate moiety is presumed to straddle the molecular mirror plane, there would appear to be no probe with which to measure its rotational barrier in (tetracyclone) $\text{Rh}(\text{acac})$. The X-ray crystal structure of **11** is shown in Figure 4a and shows that the molecule adopts a head-to-tail dimeric arrangement in which the rhodium in one monomer lies only 2.39(1) Å from the γ -carbon of the other acac ligand. The interplanar angle between the cyclopentadienone and Rh–acac rings in **11** is $\sim 65^\circ$, and the peripheral phenyls do not adopt a propeller conformation but rather a “cup-shaped” geometry (Figure 4b), as previously found¹ for the $[(\text{C}_4\text{Ph}_4\text{C}=\text{O})\text{Mo}(\text{CO})_3]$ dimeric complex **12**, depicted in Scheme 2.

Dimeric metal–acetylacetonate structures of this type were first reported for $[\text{Me}_3\text{Pt}(\text{acac})]_2$ ²⁸ and have since been found for $[(\text{C}_5\text{Me}_5)\text{Ru}(\text{acac})]_2$ ²⁹ and for $\{[(\text{C}_5\text{Me}_5)\text{Rh}(\text{acac})]_2\}^{2+}$.³⁰ In the latter case, the Rh– γ -carbon distance of 2.287(6) Å is significantly shorter than the 2.39(1) Å value found in **11**, presumably attributable to the cationic nature of the rhodium center. Kölle has

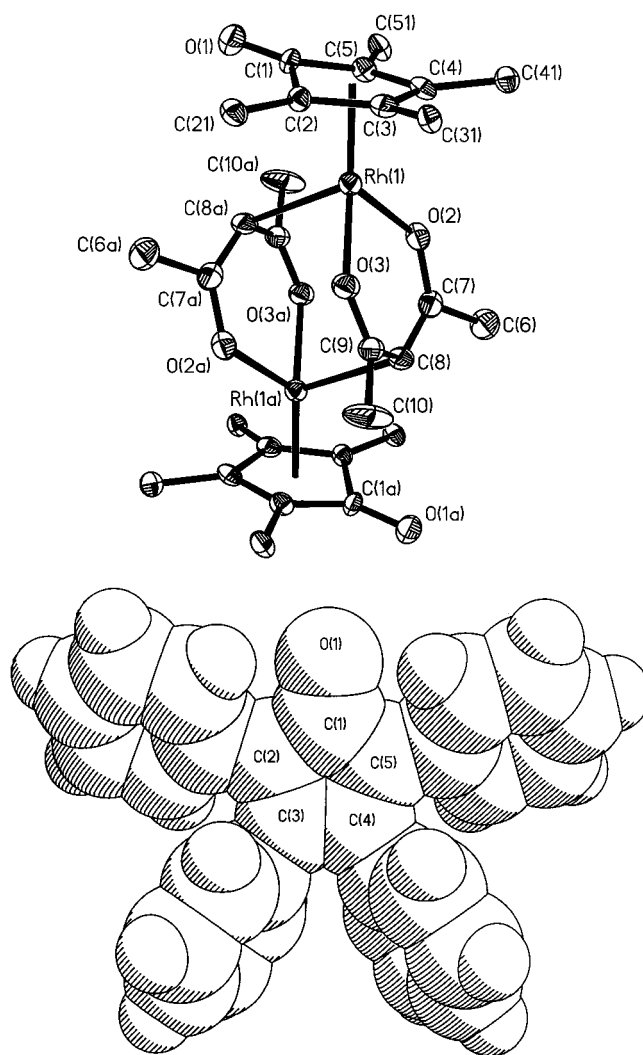


Figure 4. (a, top) Molecular structure of the dimer $[(\text{C}_4\text{Ph}_4\text{C}=\text{O})\text{Rh}(\text{acac})]_2$ (**11**; 25% thermal ellipsoids), showing only the *ipso* carbons of the peripheral phenyl rings. Hydrogen atoms are omitted for clarity. (b, bottom) Bird's eye view of a tetraphenylcyclopentadienone ring in **11**, showing the “cup-shaped” arrangement of the phenyl rings.

discussed the monomer–dimer equilibrium in $\text{Cp}^*\text{Ru}(\text{benzyl-acac})$, **13**, and has noted that the ^{13}C NMR shifts of the acac γ -carbon change very little compared to those in monomeric $\text{Ru}(\text{II})$ -acac complexes.³¹

The reaction of $(\text{acac})\text{Rh}(\text{C}_2\text{H}_4)_2$ with **2** furnished the ferrocenyl complex **14**, whose structure appears in Figure 5. As with the $\text{Fe}(\text{CO})_3$ analogue **7**, the presence of the bulky ferrocenyl substituent (which lies almost coplanar with the central ring) distorts the phenyl orientations away from the normal propeller conformation. The $(\text{acac})\text{Rh}$ ring lies almost orthogonal to the plane defined by $\text{C}(2)$ – $\text{C}(5)$ —the interplanar angle is 88° —and also to the line containing the ketonic linkage. The rhodium is essentially in a conventional square-planar environment with rhodium–diene carbon distances ranging from 2.098(5) to 2.165(6) Å; as with **3**, **7**, and **11**, the $\text{M}\cdots\text{C}=\text{O}$ distance is markedly longer

(28) (a) Hargreaves, R. N.; Truter, M. R. *J. Chem. Soc. A* **1969**, 2282. (b) Kite, K.; Psaila, A. F. *J. Organomet. Chem.* **1992**, 441, 159.

(29) (a) Kölle, U.; Kossakowski, J.; Raabe, G. *Angew. Chem., Int. Ed. Engl.* **1990**, 29, 773. (b) Smith, M. E.; Hollander, F. J.; Andersen, R. A. *Angew. Chem., Int. Ed. Engl.* **1993**, 32, 1294.

(30) Rigby, W.; Lee, H.-B.; Bailey, P. M.; McCleverty, J. A.; Maitlis, P. M. *J. Chem. Soc., Dalton Trans.* **1979**, 387.

(31) Kölle, U.; Rietmann, C.; Raabe, G. *Organometallics* **1997**, 16, 3273. In this paper it is reported that interconversion of four isomers of $\text{Cp}^*\text{Ru}(\text{benzyl-acac})$ (**13**) occurs through monomerization; we are entirely in accord with this mechanistic proposal but note that the dimers can exist in only *d,l* (*C*₂) and *meso* (*C*) forms.

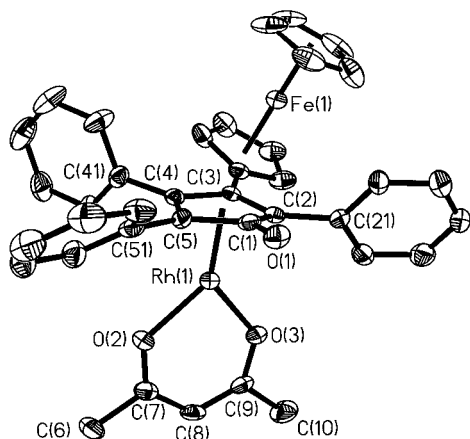


Figure 5. Molecular structure of $(C_4Ph_3FcC=O)Rh(acac)$ (**14**; 25% thermal ellipsoids), with hydrogen atoms omitted for clarity.

(Rh–C(1) = 2.380(6) Å), and the ketonic moiety is bent *exo* through 13°. In contrast to the dimeric structure of $(C_4Ph_4C=O)Rh(acac)$ (**11**), the ferrocenyl analogue **14** is clearly monomeric; the closest distance of approach between Rh and a γ -carbon of another acetylacetonate ligand is 3.73 Å, clearly too long to represent a viable bonding interaction.

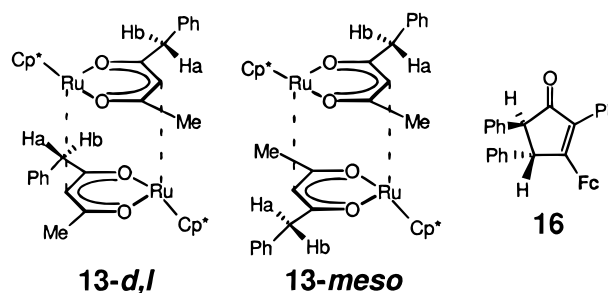
Interestingly, EHMO calculations reveal that the HOMO of $(C_4H_4C=O)Rh(acac)$ is very heavily localized on the metal, and the question arises as to the preferred site of electrophilic attack on such a system. It is known^{8b} that protonation of (tetracyclone)Co(C_5H_5) occurs at the ketonic oxygen to yield the cobaltocenium salt $[(C_5Ph_4OH)Co(C_5H_5)]^+$ (**15**), shown in Scheme 2.

The presence of the ferrocenyl group in **14** lowers the molecular symmetry such that the methyl groups of the acetylacetonate ring are no longer NMR-equivalent under conditions of slowed rotation. This results in the observation of two methyl signals in both the 1H and ^{13}C regimes at low temperature; peak coalescence data yield a barrier of 12.5 ± 0.5 kcal mol⁻¹, somewhat higher than the 8–9 kcal mol⁻¹ value estimated from our EHMO calculations. We are unaware of any previously measured rotational barriers in (cyclopentadienone)Rh(acac) systems, but values of 11–12 kcal mol⁻¹ have been reported for [tetrakis(trifluoromethyl)cyclopentadienone]M(CO)₃, where M = Fe, Ru.³²

Mass Spectra. Tetrasubstituted cyclopentadienones have been the subject of detailed mass spectral studies. The facile loss of CO to yield radical cations of the type $[C_4Ar_4]^+$ led to much speculation as to the structure of this species: i.e., whether it adopted a square-planar (cyclobutadiene) or a tetrahedral geometry. This ion dissociates to yield the appropriately substituted $[ArC \equiv CAr']^+$ fragments, but careful labeling experiments demonstrated the formation of alkynes that would have been “diagonally related” in the square-planar precursor; it was therefore concluded that $[C_4Ar_4]^+$ radical cations are tetrahedral.³³

The electron impact mass spectrum of $(C_4Ph_4C=O)Rh(acac)$ (**11**) shows a parent peak (m/z 586) and a fragment at m/z 558 assignable to $[(C_4Ph_4)Rh(acac)]^+$;

Chart 2



however, there was also a much more intense peak at m/z 279 for the corresponding doubly charged species $[(C_4Ph_4)Rh(acac)]^{2+}$. In this latter ion, one could assign a formal charge of +3 to the rhodium atom, in keeping with its normal chemical behavior. Similarly, there are peaks at m/z values of 459 and 229.5 for $[(C_4Ph_4)Rh]^+$ and $[(C_4Ph_4)Rh]^{2+}$, respectively. This phenomenon is even more evident in the ferrocenyl analogue **14**, for which the $[M - CO]^+$ fragment at m/z 666 is barely detectable, yet the doubly charged ion at m/z 333, assignable to $[(C_4Ph_3Fc)Rh(acac)]^{2+}$, is a major peak. One can speculate whether the second ionization occurs at rhodium or at iron, and electrochemical measurements on these complexes are in progress. Interestingly, the mass spectra of **11** and **14** do not give rise to fragment ions of the type $[C_4Ph_3R]^+$, where R is phenyl or ferrocenyl.

Concluding Remarks. One of our longer term goals involves using the presence of the organometallic moiety to control the site of nucleophilic attack on the cyclopentadienone ring system, and the reactions with alkynyl Grignard reagents or C_6F_5Li will be the subject of a future report.

Finally, we note that reactions involving 3-ferrocenyl-2,3,4-triphenylcyclopentadienone (**2**) frequently yield, after chromatographic separation of the products, small quantities of a compound of formula $(C_4H_2Ph_3FcC=O)$. This dihydro complex, resulting from incomplete oxidation of the mixed benzoin derived from benzaldehyde and formylferrocene, has now been characterized as 3-ferrocenyl-2,4,5-triphenylcyclopent-2-en-1-one (**16**). Its identification as the isomer with two hydrogens attached to *adjacent* phenyl-bearing carbons is evident from the 1H NMR spectrum, which exhibits two sets of doublets ($J = 1.9$ Hz) at δ 4.46 and 3.67. The magnitude of the coupling between these protons suggests a dihedral angle between them of $\sim 90^\circ$, i.e. a diequatorial arrangement, as shown for **16** (Chart 2). Moreover, in the 1H – 1H COSY spectrum, each of these hydrogens is clearly coupled to the ortho protons of its neighboring phenyl ring. These data match closely the NMR parameters for 2,3,4,5-tetraphenylcyclopent-2-en-1-one,³⁴ prepared by reduction of tetracyclone.³⁵

Experimental Section

General Methods. All reactions were carried out under an atmosphere of dry nitrogen employing conventional benchtop and glovebag techniques. All solvents were dried according to

(32) Kruczynski, L.; Martin, J. L.; Takats, J. *J. Organomet. Chem.* **1974**, *80*, C9.

(33) Bursey, M. M.; Harvan, D. J.; Hass, J. R. *Org. Mass Spectrom.* **1985**, *20*, 197 and references therein.

(34) The 1H NMR spectrum of 2,3,4,5-tetraphenylcyclopent-2-en-1-one exhibits doublets ($J = 2.6$ Hz) at δ 4.65 and 3.75.

(35) Brown, D. A.; Hargaden, J. P.; McMullin, C. M.; Gogan, N.; Sloan, H. *J. Chem. Soc.* **1963**, 4914.

standard procedures before use.³⁶ Silica gel (particle size 20–45 μm) was employed for flash column chromatography. ^1H and ^{13}C solution NMR spectra were acquired on a Bruker DRX 500 spectrometer and were referenced to the residual proton signal or the ^{13}C solvent signal. Mass spectra were determined using a Finnigan 4500 spectrometer by direct electron impact (DEI) or direct chemical ionization (DCI) with NH_3 . Infrared spectra were recorded on a Bio-Rad FTS-40 spectrometer. Melting points (uncorrected) were determined on a Thomas-Hoover melting point apparatus. Elemental analyses were performed by Guelph Chemical Laboratories, Guelph, Ontario, Canada.

3-Ferrocenyl-2,4,5-triphenylcyclopentadienone (**2**)^{19,37} and (tetraphenylcyclopentadienone)tricarbonyliron (**3**)²⁷ were prepared by literature methods.

(3-Ferrocenyl-2,4,5-triphenylcyclopentadienone)tricarbonyliron (7). 3-Ferrocenyl-2,4,5-triphenylcyclopentadienone (0.246 g, 0.5 mmol) and $\text{Fe}_2(\text{CO})_9$ (0.182 g, 0.5 mmol) were stirred under reflux in THF (20 mL) for 4 h. The reaction mixture was cooled to room temperature, reduced to half its volume under reduced pressure, and then treated with hexane (15 mL). The dark brown precipitate was filtered, dried under vacuum, and recrystallized from CH_2Cl_2 /hexane (1:1) to give **7** (0.183 g, 0.29 mmol; 58%) as dark red crystals, mp 210 $^\circ\text{C}$. ^1H NMR (500 MHz, CD_2Cl_2): δ 7.7–7.1 (m, 15H phenyl rings), 4.1* (m, 2H, C_5H_4), 4.08 (s, 5H, C_5H_5), 4.06 (m, 2H, C_5H_4), 3.92* (s, 5H, C_5H_5), 3.84 (m, 1H, C_5H_4), 3.76 (m, 1H, C_5H_4), 3.57* (m, 1H, C_5H_4), 3.50* (m, 1H, C_5H_4). Ferrocenyl peaks for the major isomer (~80%) are marked by asterisks. ^{13}C NMR (125 MHz, CD_2Cl_2): δ 208.77 (Fe–CO), 171.79 (CO), 133.2–127.3 (phenyl C's), 99.88, 91.30, 86.49, 81.90 (central ring C's), 73.90 (1 CH), 70.74* (2 CH's), 70.65 (C_5H_5), 70.34* (C_5H_5), 69.25* (2 CH's), 69.00 (1 CH), 64.34 (1 CH), 63.58 (1 CH). Ferrocenyl peaks for the major isomer (~80%) are marked by asterisks; at 177 K, Fe– ^{13}C O resonances are observed at δ 209.1, 207.2, and 207.0. IR (CH_2Cl_2): ν_{CO} at 2067, 2012, and 1636 cm^{-1} . MS (DEI; m/z (%)): 632 [M]⁺ (8), 548 [$\text{M} - 3\text{CO}$]⁺ (15), 520 [$\text{M} - 4\text{CO}$]⁺ (12), 492 [$\text{M} - \text{Fe}(\text{CO})_3$]⁺ (17), 427 [$\text{M} - \text{Fe}(\text{CO})_3 - \text{C}_5\text{H}_5$]⁺ (17), 399 [$\text{M} - \text{Fe}(\text{CO})_4 - \text{C}_5\text{H}_5$]⁺ (11), 342 [$\text{M} - \text{Fe}(\text{CO})_4 - \text{Fe}(\text{C}_5\text{H}_5)$]⁺ (60), 286 [$(\text{C}_6\text{H}_5\text{C}\equiv\text{CC}_5\text{H}_4)\text{Fe}(\text{C}_5\text{H}_5)$]⁺ (70), 165 [$\text{C}_6\text{H}_5\text{C}\equiv\text{CC}_5\text{H}_4$]⁺ (15), 121 [$\text{C}_5\text{H}_5\text{Fe}$]⁺ (100), 56 [Fe]⁺ (15). Anal. Calcd for $\text{C}_{36}\text{H}_{24}\text{Fe}_2\text{O}_4$ C, 68.39, H, 3.83. Found, C, 67.85; H, 3.93.

(Acetylacetonato)(3-ferrocenyl-2,4,5-triphenylcyclopentadienone)rhodium(I) (14). To a solution of 3-ferrocenyl-2,4,5-triphenylcyclopentadienone (0.246 g, 0.5 mmol) in THF (10 mL) was added dropwise a solution of $(\text{acac})\text{Rh}(\text{C}_2\text{H}_4)_2$ (0.128 g, 0.5 mmol) in THF (10 mL), and the mixture was stirred under reflux for 4 h, after which time the color had changed from deep blue to purple-red. The reaction mixture was cooled to room temperature, reduced to half its volume under reduced pressure, and then treated with hexane (10 mL). The dark red precipitate was filtered, dried under vacuum, and recrystallized from CH_2Cl_2 /hexane (1:1) to give **14** (0.17 g, 0.25 mmol; 49%) as burgundy red crystals, mp 169 $^\circ\text{C}$. ^1H NMR (500 MHz, CD_2Cl_2): δ 8.05–7.15 (m, 15H phenyl rings), 5.48 (s, 1H, γ -CH of acac), 4.18 (m, 2H, C_5H_4), 4.03 (t, 1H, C_5H_4), 3.86 (s, 5H, C_5H_5), 3.77 (t, 1H, C_5H_4), 2.16 (s, 6H, 2 CH_3 's); at 198 K, CH₃'s at δ 2.09 and 2.05. ^{13}C NMR (125 MHz, CD_2Cl_2): δ 187.49 (C=O), 163.14 (2 CO's in acac), 133.5–127.9 (phenyl C's), 99.59 (γ -CH of acac), 72.60, 71.12, 70.66, 70.42 (CH's of C_5H_4), 69.99 (C_5H_5), 27.46 (2 CH_3 's); at 198 K, CH₃'s at δ 27.41 and 27.05. IR (CH_2Cl_2): ν_{CO} at 1635 cm^{-1} . MS (DEI; m/z (%)): 694 [M]⁺ (5), 666 [$\text{M} - \text{CO}$]; ($\text{C}_6\text{Ph}_3\text{Fc})\text{Rh}(\text{acac})$]⁺ (1), 333 [$(\text{C}_4\text{Ph}_3\text{Fc})\text{Rh}(\text{acac})$]²⁺ (16), 168 [$(\text{C}_5\text{H}_5)\text{Rh}$]⁺ (6), 165 [$\text{C}_6\text{H}_5\text{C}\equiv\text{CC}_5\text{H}_4$]⁺ (20), 84 [$(\text{C}_5\text{H}_5)\text{Rh}$]²⁺ (63), 43 [CH_3CO]⁺ (100). MS (DCI; m/z (%)): 695 [$\text{M} + \text{H}$]⁺ (5), 255

[$\text{C}_3\text{Ph}_2\text{C}_5\text{H}_5$]⁺ (37), 118 [$\text{Hacac} + \text{NH}_4$]⁺ (30), 101 [$\text{Hacac} + \text{H}$]⁺ (50). Anal. Calcd for $\text{C}_{38}\text{H}_{31}\text{FeRhO}_3$: C, 65.70; H, 4.50. Found: C, 61.30, 61.36; H, 4.52, 4.31. (Repeated analyses on crystalline samples gave a consistently low carbon percentage.)

(Acetylacetonato)(tetraphenylcyclopentadienone)rhodium(I) (11). As for **14**, tetracyclone (0.384 g, 1.0 mmol) and $(\text{acac})\text{Rh}(\text{C}_2\text{H}_4)_2$ (0.258 g, 1.0 mmol) in THF (40 mL) yielded **11** (0.41 g, 0.70 mmol; 70%) as dark red crystals, mp 260 $^\circ\text{C}$ dec (lit.⁹ mp 255–270 $^\circ\text{C}$). ^1H NMR (500 MHz, CD_2Cl_2): δ 7.8–7.1 (m, 20H, phenyl rings), 5.45 (s, 1H, γ -CH of acac), 2.09 (s, 6H, 2 CH_3 's). ^{13}C NMR (125 MHz, CD_2Cl_2): δ 187.72 (C=O), 163.24 (2 CO's in acac), 131.5, 131.4, 131.2, 131.0, 128.7, 128.3, 128.1 (phenyl C's), 99.46 (γ -CH of acac), 27.38 (2 CH_3 's). IR (CH_2Cl_2): ν_{CO} at 1635 cm^{-1} . MS (DEI; m/z (%)): 586 [M]⁺ (11), 558 [$\text{M} - \text{CO}$]; (C_4Ph_4) $\text{Rh}(\text{acac})$]⁺ (8), 486 [$\text{M} - \text{Hacac}$]⁺ (17), 459 [$(\text{C}_4\text{Ph}_4)\text{Rh}$]⁺ (15), 380 [$(\text{C}_2\text{Ph}_2)\text{Rh}(\text{acac})$]⁺ (10), 279 [$(\text{C}_4\text{Ph}_4)\text{Rh}(\text{acac})$]²⁺ (50), 229.5 [$(\text{C}_4\text{Ph}_4)\text{Rh}$]²⁺ (3), 178 [$\text{PhC}\equiv\text{CPh}$]⁺ (55), 103 [Rh]⁺ (50), 43 [CH_3CO]⁺ (100). MS (DCI; m/z (%)): 587 [$\text{M} + \text{H}$]⁺ (100), 178 [$\text{C}_6\text{H}_5\text{C}\equiv\text{CC}_6\text{H}_5$]⁺ (7), 118 [$\text{Hacac} + \text{NH}_4$]⁺ (25), 101 [$\text{Hacac} + \text{H}$]⁺ (50).

3-Ferrocenyl-2,4,5-triphenylcyclopent-2-en-1-one (16). During the chromatographic separation of pure **2**, minuscule quantities of **16** were consistently obtained as a red solid, mp 141 $^\circ\text{C}$. ^1H NMR (500 MHz, CD_2Cl_2): δ 7.7–7.2 (m, 15H phenyl rings), 4.46 (d, 1H, $J = 1.9$ Hz), 4.31 (m, 2H, C_5H_4), 4.13 (m, 2H, C_5H_4), 4.02 (s, 5H, C_5H_5), 3.67 (d, 1H, $J = 1.9$ Hz). ^{13}C NMR (125 MHz, CD_2Cl_2): δ 171.16 (CO), 143.88, 140.54, 138.36, 133.62, 129.54, 129.22, 129.03, 128.62, 128.08, 127.49, 127.21, 127.11, 126.97 (phenyl C's), 71.33, 71.13, 71.00 (C_5H_4), 69.97 (C_5H_5), 62.86 (CH), 57.92 (CH). IR (CH_2Cl_2): ν_{CO} at 1687 cm^{-1} . MS (DEI; m/z (%)): 494 [M]⁺ (100); 429 [$\text{M} - \text{C}_5\text{H}_5$]⁺ (5); 178 [$\text{C}_6\text{H}_5\text{C}\equiv\text{CC}_6\text{H}_5$]⁺ (7), 165 [$\text{C}_6\text{H}_5\text{C}\equiv\text{CC}_5\text{H}_4$]⁺ (10), 121 [$\text{C}_5\text{H}_5\text{Fe}$]⁺ (20); 56 [Fe]⁺ (32). MS (DCI; m/z (%)): 495 [$\text{M} + \text{H}$]⁺ (100). Anal. Calcd for $\text{C}_{33}\text{H}_{26}\text{FeO}$: C, 80.14; H, 5.30. Found: C, 80.26; H, 5.42.

Crystallographic Data for 3, 7, 11, and 14. X-ray crystallographic data for **3**·THF, **7**· H_2O , and **14** were each collected from a suitable sample mounted with epoxy on the end of a thin glass fiber. Data were collected on a P4 Siemens diffractometer equipped with a Siemens SMART 1K CCD area detector (employing the program SMART³⁸) and a rotating anode utilizing graphite-monochromated Mo K α radiation ($\lambda = 0.71073$ Å). Data processing was carried out by use of the program SAINT,³⁹ while the program SADABS⁴⁰ was utilized for the scaling of diffraction data, the application of a decay correction, and an empirical absorption correction based on redundant reflections. Structures were solved by using the direct-methods procedure in the Siemens SHELXTL⁴¹ program library and refined by full-matrix least-squares methods on F^2 . All non-hydrogen atoms (with the exception of the carbon atoms of the tetrahydrofuran solvate in **3**·THF) were refined using anisotropic thermal parameters. Hydrogen atoms were added as fixed contributors at calculated positions, with isotropic thermal parameters based on the carbon atom to which they are bonded. In the course of the refinement process, a solvated molecule of tetrahydrofuran was located in the asymmetric unit of **3**; similarly, a single water molecule was located in the asymmetric unit of **11**. Although in both cases the diffraction data readily allowed for a complete anisotropic refinement of the target molecule, a satisfactory refinement of the solvate atomic positions proved more difficult to obtain, leading to rather high values for the residual electron density

(38) Sheldrick, G. M. SMART, Release 4.05; Siemens Energy and Automation Inc., Madison, WI 53719, 1996.

(39) Sheldrick, G. M. SAINT, Release 4.05; Siemens Energy and Automation Inc., Madison, WI 53719, 1996.

(40) Sheldrick, G. M. SADABS (Siemens Area Detector Absorption Corrections); Siemens Energy and Automation Inc., Madison, WI 53719, 1996.

(41) Sheldrick, G. M. SHELXTL, Version 5.03; Siemens Crystallographic Research Systems, Madison, WI, 1994.

(36) Perrin, D. D.; Armarego, W. L. F.; Perrin, D. R. *Purification of Laboratory Chemicals*, 2nd ed.; Pergamon Press: New York, 1980.

(37) Rausch, M. D.; Siegel, A. *J. Org. Chem.* **1968**, *33*, 4545.

(concentrated primarily in the region of the solvent molecules) and the refinement statistics associated with these crystal structures.

Molecular Orbital Calculations. These calculations were performed within the extended Hückel formalism using weighted H_{ij} values,⁴² by using the program CACAO.⁴³ The molecular geometries were idealized versions taken from the X-ray crystal structures of **3** and **11**.

NMR Simulations. These simulations were carried out by using the multisite EXCHANGE program generously provided by Professor R. E. D. McClung (University of Alberta at Edmonton).

(42) (a) Hoffmann, R. *J. Chem. Phys.* **1963**, *39*, 1397. (b) Hoffmann, R.; Lipscomb, W. N. *J. Chem. Phys.* **1962**, *36*, 2179, 3489. (c) Ammeter, J. H.; Bürgi, H.-B.; Thibeault, J. C.; Hoffmann, R. *J. Am. Chem. Soc.* **1978**, *100*, 3686.

(43) (a) CACAO, Version 5.0; 1998. (b) Mealli, C.; Proserpio, D. M. *J. Chem. Educ.* **1990**, *67*, 399.

Acknowledgment. Financial support from the Natural Sciences and Engineering Council of Canada and from the Petroleum Research Fund, administered by the American Chemical Society, is gratefully acknowledged. M.S. thanks the NSERC for a Graduate Fellowship and McMaster University for a Centennial scholarship. Mass spectra were acquired courtesy of Dr. Kirk Green of the McMaster Regional Mass Spectrometry Centre.

Supporting Information Available: Tables of crystal data, atomic parameters, bond lengths and angles, anisotropic displacement parameters, and hydrogen coordinates for **3**, **7**, **11**, and **14**. This material is available free of charge via the Internet at <http://pubs.acs.org>.

OM990559B